Electron guiding center modeling for Hall thruster simulations

IEPC-2009-69

Presented at the 31st International Electric Propulsion Conference,
University of Michigan, Ann Arbor, Michigan, USA
September 20–24, 2009

Jan Miedzik* and Serge Barral†
Institute of Plasma Physics and Laser Microfusion, 01-497 Warsaw, Poland

and

Stéphan Zurbach‡
Snecma, Safran Group, 27208 Vernon, France

A one-dimensional Quasineutral Particle In Cell (QPIC) simulation of the plasma along a field line in a Hall thruster is investigated, assuming a guiding center model of electron motion. The influence of magnetic mirror effects on the electric field is assessed numerically for different magnetic field and ion density profiles. These results suggests that the Boltzmann relation used in hybrid models generally fails to provide a reasonable estimate of the electric field along field lines, even in the absence of magnetic field gradient. The inclusion of the magnetic gradient force in Boltzmann relation mitigates this issue but remains too crude an approximation to quantitatively estimate the electric field in typical Hall thruster magnetic configurations. Finally, simulations suggests that the centrifugal force acting on electrons in actual axisymmetric geometries contributes only marginally to the ambipolar field.

Nomenclature

$\mathbf{b}$	Unit vector along $\mathbf{B}$, $\mathbf{b} \equiv \mathbf{B}/B$	$u_\parallel$	Electron guiding center velocity along $\mathbf{B}$
$\mathbf{B}$, B	Magnetic field (vector, magnitude)	$\mathbf{u}_\perp$	Electron guiding center velocity perpendicular to $\mathbf{B}$
e	Absolute electron charge	$\mathbf{v}$	Electron velocity vector
$E_\parallel$	Electric field along $\mathbf{B}$	$v_\perp$	Electron velocity in the drifting frame
$E_\perp$	Electric field perpendicular to $\mathbf{B}$	$\mathbf{v}_E$, v_E	Electron drift velocity, $\mathbf{v}_E \equiv \mathbf{E} \times \mathbf{B}$
j_{ew}	Current density of electrons impinging walls	ϕ	Plasma potential
j_{iw}	Current density of ions impinging walls	Φ_w	Potential drop across the wall sheath
m_e	Electron mass	κ	Boltzmann constant
n_e	Density of electrons	μ	Electron magnetic moment, $\mu \equiv \frac{1}{2} m_e v_\perp^2 / B$
n_i	Density of ions	$\bar{\mu}$	Average magnetic moment of all electrons
n_n	Density of neutrals	ν	Momentum transfer frequency for electrons
r	Radial coordinate, $r \equiv \zeta + const$	ω_{ce}	Electron cyclotron frequency
T_e	Total electron temperature	σ	Secondary emission yield
$T_{e\parallel}$	Electron temperature along $\mathbf{B}$	ζ	Field line curvilinear coordinate
$T_{e\perp}$	Electron temperature perpendicular to $\mathbf{B}$		

*PhD student, Division of Magnetised Plasma, jmiedzik@ipilm.waw.pl.
†Assistant Professor, Division of Magnetised Plasma, sbarral@ifpilm.waw.pl.
‡R & D Engineer, Space Engines Division, stephan.zurbach@snecma.fr.

I. Introduction

A rich variety of Hall thrusters simulations has emerged in the past 15 years, ranging from fully fluid quasineutral steady 1D models to fully kinetic transient 3D models. Owing to the balanced compromise they offer between description accuracy, manageability and computational requirements, 2D quasineutral hybrid models have become the tool of choice for many engineering applications. A severe shortcoming of hybrid simulations resides, however, in their incapacity to describe the influence of magnetic field gradient forces on the electron dynamics. Several studies have underlined the role of magnetic mirrors in the confinement of the plasma away from the walls and in the ion beam focusing.[1–4] The role of the centrifugal force induced by the drifting motion of electrons in a cylindrical geometry has also been pointed out.[5] Magnetic mirroring and finite curvature effects are yet more stringent in small Hall thrusters, in cylindrical Hall thrusters and in the closely related HEMP thrusters.[3]

The literature does not always provide, however, a consistent and accurate picture of the effect of magnetic mirrors. Many authors have for instance stated that magnetic gradients do not affect Boltzmann relation,

$$\kappa T_e \frac{\partial n_e}{\partial \zeta} - n_e e \frac{d\phi}{d\zeta} = 0. \tag{1}$$

M. Keidar and I. D. Boyd have acknowledged the effect of magnetic field gradients and have proposed the relation[2]

$$\frac{\partial}{\partial \zeta}\left(n_e \kappa T_e\right) + n_e \frac{\kappa T_e}{B}\frac{\partial B}{\partial \zeta} - n_e e \frac{d\phi}{d\zeta} = 0. \tag{2}$$

The above relation relies, however, on a somewhat inconsistent set of assumption: the mirror force term assumes strong anisotropy for the electron pressure tensor ($T_{e\perp} \approx T_e \gg T_{e\parallel}$), and yet the pressure gradient term implicitly assumes $T_{e\parallel} \approx T_e$. Indeed, neglecting the centrifugal force and the net electron current along field lines, the actual momentum conservation law along B reads:[6]

$$\frac{\partial}{\partial \zeta}\left(n_e \kappa T_{e\parallel}\right) + n_e \frac{\kappa T_{e\perp} - \kappa T_{e\parallel}}{B}\frac{\partial B}{\partial \zeta} - n_e e \frac{d\phi}{d\zeta} = 0, \tag{3}$$

which cannot, in principle, be reduced to Eq. (2). This law also clearly shows that Boltzmann relation does not hold in the case where the electron temperature anisotropy is significant, which is precisely what one expects in the acceleration region of Hall accelerators. The study of magnetic mirrors appears therefore very difficult to approach from a purely analytical viewpoint, and no obvious way exists to account for such effects in hybrid simulations where only the total temperature of electrons is known.

Magnetic gradient effects can be efficiently modeled, however, using a recently devised method whereas the quasineutrality assumption and the Guiding Center (GC) approximation for electron motion are combined.[6,7] Although the method is computationally more intensive than hybrid modeling, it remains orders of magnitude lighter than full-fledged kinetic-Poisson simulations, making it a most relevant choice for an engineering simulation tool. Added to this, the particle description used by this method easily lends itself to parallelization, allowing it to take full advantage of the current trend towards affordable multiprocessing.

The present paper reports on an ongoing effort to adapt the combined GC/Quasineutral Particle-In-Cell (GC-QPIC) method[6,7] for the purpose of Hall thruster modeling. Although the model is ultimately intended to resolve an axisymmetric 2D domain, the present investigations shall be limited to the case of a single magnetic field line in slab or cylindrical geometries. The simulation assumes an imposed distribution of ions and a given electric field $E_\perp$ across magnetic lines. The electric field $E_\parallel$ along the magnetic field and the electron distribution function (given in terms of guiding center variables) are solved self-consistently. The model takes into account electron-neutral collisions in the bulk as well as a self-consistent model of the wall sheath for electron-wall collisions. After an assessment of its proper convergence in a typical case, we shall use the model to discuss the influence of magnetic mirrors and of the centrifugal force on the ambipolar field along the magnetic field. The results are compared to the classical isothermal Boltzmann relation, Eq. (1), which is used in hybrid model to estimate the electric field along **B**.

II. Physical and numerical model

A. Motivations and prior art

To the best of our knowledge, the QPIC formalism has never been considered within the context of Hall discharges while the GC approximation has only been used sparsely in some analytical studies. There exists, however, a large

body of literature on kinetic-Poisson simulations, where the electric field is computed from Poisson equation and where the dynamics of electrons directly follows the Lorentz force law. The drawbacks of such simulations are well-known, namely:

- very high computational requirements due to the need to resolve the plasma frequency, the electron cyclotron frequency and the spatial scale associated with the Debye length; the use of implicit integration can somewhat relax the condition on time and space discretization,[8] but the cyclotron motion must still be resolved,
- the necessity to modify physical constants and/or geometrical parameters to perform simulations with reasonable resources and within a reasonable time frame; common modifications of the physical constants include alterations of the space permittivity and of the ion-to-electron mass ratio;[9,10] common modifications of the geometry include domain downscaling[11] and reduction to a domain subset.[8]

It is worth noting that the phenomena taking place at the Debye length scale and at the plasma frequency are improperly described by most such simulations, either as a result of implicit integration or of physical constants alteration. It would appear more sensible, therefore, to assume *a priori* electric quasineutrality rather than to rely on Poisson equation, thus removing any related discretization constraint. This idea is central to many fluid and hybrid simulations, but its practical implementation in PIC electron simulations is relatively new.[7]

The GC approximation reposes in turn on the fact that for electron cyclotron radii smaller than the characteristic gradient length of the E and B fields, the trajectory of the electron guiding center can be effectively decoupled from the cyclotron rotation. Combined with the QPIC formalism, the GC approximation offers the following advantages:

- the constraint on the time step is strongly relaxed, because the cyclotron motion does not need to be resolved and the time step is limited only by the CFL condition with respect to the guiding center velocity
- in the common case where the statistical angular distribution of electrons with respect to their guiding centers is uniform, the phase space can be reduced by one dimension through a substitution of the velocity vector $\mathbf{v} = (v_{ex}, v_{ey}, v_{ez})$ by a parameterization in terms of the magnetic moment μ and of the velocity $u_\parallel$ along magnetic field lines,
- several numerical optimizations are made possible by decoupling the motion along and across fields lines, taking advantage of the fact that guiding center trajectories approximately follow field lines.

B. Governing equations

This work constitutes a preliminary assessment of the GC approximation in Hall thrusters, limited to the simulation of a single magnetic field line in slab and axisymmetric configurations, accounting for possible field line curvature and magnetic gradients. The profiles $B(\zeta)$, $E_\perp(\zeta)$ and $n_i(\zeta)$ are considered inputs of the model. The electric field $E_\parallel(t,\zeta)$ and the electron distribution $f_e\left(t,\zeta,u_\parallel,\mu\right)$ are determined self-consistently so as to maintain quasineutrality with the ion background. The assumption of a steady ion background is justified in view of the fact that the dynamics of electrons along the field lines is substantially faster than the variations of density induced by the dynamics of ions.

The numerical integration of the classical equation of motion for electrons in electric and magnetic fields, namely

$$m_e \frac{d\mathbf{v}}{dt} = -e\left(\mathbf{E} + \mathbf{v}\times\mathbf{B}\right), \tag{4}$$

limits the integration time step to $\Delta t \ll \frac{1}{\omega_{ce}}$. This constrain can be avoided by the use of the GC approximation, in which only the motion of the guiding center electrons is resolved. In many cases, the orbital angles of electrons are equidistributed and one can reduce the electron phase space to variables $u_\parallel$, μ, whereas the latter is at the leading order (*i.e.* for infinitely small gyroradius) a constant of motion in slowly changing fields. In cylindrical geometry and in the absence of azimuthal fields ($B_\theta = E_\theta = 0$), the leading order equations for the motion of the guiding center read,

$$\frac{du_\parallel}{dt} = -\frac{e}{m_e}E_\parallel - \mu\frac{dB}{d\zeta} + \frac{v_E^2}{r}b_r, \tag{5}$$

$$\mathbf{u}_\perp = \mathbf{v}_E, \tag{6}$$

where the right hand side of Eq. (5) sums the contributions of the electrostatic field, of the magnetic mirror force and of the centrifugal force, with b_r the projection of $\mathbf{b}$ on the radial axis. Unlike the mirror force, the centrifugal force

acts uniformly on all electrons notwithstanding their kinetic state, making it possible to integrate this force into an "effective" electric field,

$$\tilde{E}_{\parallel} \equiv E_{\parallel} - \frac{m_e}{e}\frac{v_E^2}{r} b_r. \tag{7}$$

It is readily noted that $\tilde{E}_{\parallel}$ and $E_{\parallel}$ coincide in slab geometry ($r \to \infty$).

Let us now consider the complete momentum conservation of electrons along the magnetic field lines, which generalizes the expression of J. Joyce *et al.*[7] to account for the centrifugal force,

$$-e\tilde{E}_{\parallel} = \frac{|B|}{n_e}\frac{\partial}{\partial \zeta}\left(\frac{n_e \kappa T_{e\parallel}}{|B|}\right) + \bar{\mu}\frac{\partial |B|}{\partial \zeta} + \nu_e m_e u_{e\parallel} + \frac{1}{n_e}\frac{\partial}{\partial t}\left(n_e m_e u_{e\parallel}\right). \tag{8}$$

While this equation does not by itself enforce quasineutrality, a simple modification was suggested by J. Joyce *et al.*[7] to ensure that quasineutrality is satisfied in the steady state. The altered version of the above equation used in the QPIC method to estimate the electric field along field lines reads,

$$-e\tilde{E}_{\parallel} = \frac{|B|}{n_i}\frac{\partial}{\partial \zeta}\left(\frac{n_i \kappa T_{e\parallel}}{|B|}\right) + \bar{\mu}\frac{\partial |B|}{\partial \zeta} + \nu_e m_e u_{e\parallel}, \tag{9}$$

where the density of ions n_i is used instead of n_e in the pressure term. The drag term (last term on the right hand side) is disregarded in the present model since the net current along the field lines is typically negligible, which has been verified in simulations. The electric field hence calculated can be shown to drive electrons from regions with negative space charge towards regions of positive space charge so as to restore quasineutrality.[6]

C. Sources, sinks and collisions

Whenever an electron is recombined at the walls, a new electron is introduced to restore the global neutrality over the field line. The position of the new electron on the field line is random, with all positions ζ being equiprobable. The velocity of new electrons is sampled from a Gaussian probability distribution of variance T_{e0} and their direction is determined assuming statistical spherical uniformity, from which $u_{\parallel}$ and μ are computed.

Electrons that reach the edge of a wall sheath may be reflected elastically on the sheath (which solely changes the sign of $u_{\parallel}$), or may be either backscattered or recombined at the surface if they have enough energy to cross the sheath. The simulation does not distinguish between backscattered and true secondaries and adopts at the moment a relatively crude model of electron-wall collisions where only 0 or 1 electron can be emitted, assuming a constant "secondary emission" coefficient σ. The sheath is considered perpendicular to **B**.

The sheath potential is in theory determined so as to repel enough electrons for the ion current to balance the net current of electrons at the walls. The ion current density at the sheath edge is determined from Bohm condition,

$$j_{iw} = e n_i \sqrt{\frac{\kappa T_{e\parallel}}{m_i}}. \tag{10}$$

A common choice for the computation of the sheath potential is the algorithm of Parker *et al.*[12] In this method, the number $\mathscr{N}_i$ of ions impinging the walls during a time step is determined from the above formula, and electrons impinging the wall are sorted on the basis of their velocity $u_{\parallel}$. The sheath potential is then set to the energy of the $\mathscr{N}_e$-th fastest electrons where $\mathscr{N}_e = \mathscr{N}_i/(1-\sigma)$. This algorithm ensures that the number of electrons absorbed by the walls is at any time equal to the number of ions, but we have observed that it suffers from large statistical fluctuations in the common occurrence where $\mathscr{N}_i$ is small. A method inspired from the algorithm of F. Taccogna[13] was thus preferred, where the sheath is modeled as a capacitor which potential increases whenever a negative net charge builds on the wall. The potential drop across the sheath is thus calculated from,

$$\frac{d\Phi_w}{dt} = \frac{1}{c}\left[j_{ew}(1-\sigma) - j_{iw}\right], \tag{11}$$

where c is an artificial surface capacitance and j_{ew} accounts only for electrons which velocity $u_{\parallel}$ is sufficient to overcome the sheath potential Φ_w. The capacitance is determined empirically to ensure a satisfactory damping of statistical fluctuations while keeping the accommodation time reasonably short.

The energy and direction of backscattered electrons is determined randomly by assuming that they are thermalized by the wall at a temperature T_w, with the additional condition that their energy cannot be greater than the energy of the impinging electron. These electrons then gain additional energy in the sheath and are reintroduced in the bulk with new values of $u_\parallel$ and μ.

Only elastic collisions with neutrals are considered in the bulk. A constant density of neutrals n_n is assumed, and the collision cross-sections assumed are those for electron-xenon momentum transfer from A. V. Phelps.[14] The Monte-Carlo implementation of collision events is based on the null-collision method.[15] The pre-collision kinetic state is determined from $u_\parallel$, v_E, μ and from a random gyrophase. The energy remains unchanged after the collision, but a new random direction is sampled from which the new $u_\parallel$ and μ are determined.

III. Simulation

A. Parameters

The field line is discretized into 20 cells which cross-sections varies according to the section of the magnetic flux tube, *i.e.* in inverse proportion to B. The "temperature" of the electron source is $T_{e0} = 10\,\mathrm{eV}$, the energy of secondary/backscattered electrons emitted by the walls is $T_{ew} = 5\,\mathrm{eV}$ and the secondary emission yield is $\sigma = 0.5$. The electric field perpendicular to B is set to $E_\perp = 10\,\mathrm{kV m^{-1}}$ and the density of neutrals to $10^{19}\,\mathrm{m^{-3}}$. Simulations in slab geometry assume walls at positions $\zeta = \pm 1\,\mathrm{cm}$. Simulations in axisymmetric geometry assume walls at radii $R_0 = 3\,\mathrm{cm}$ and $R_1 = 5\,\mathrm{cm}$. The various ion density profiles $n_i(\zeta)$ and magnetic field profiles $B(\zeta)$ considered in simulations are shown in the Fig. 1.

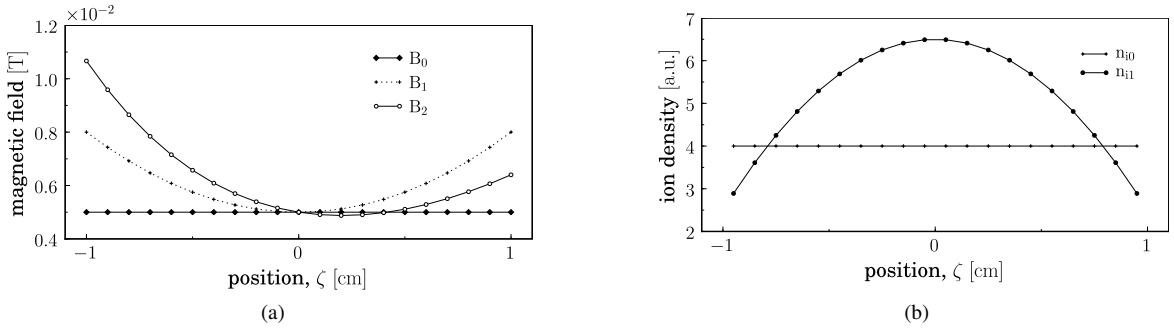

Figure 1: Profiles of (a) magnetic field and (b) ion density considered in simulations.

B. Numerical implementation

Equation (5) is integrated numerically in time using the Semi Implicit MidPoint (SIMP) pusher developed by V. Fuchs and J. P. Gunn.[16] This scheme is essentially a modified second-order Runge-Kutta scheme which, like the leapfrog scheme, is area-preserving. Unlike the leapfrog scheme, however, it allows both the velocity and the position to be known at the same instants, which for the QPIC method is essential to evaluate the electric field. The application of the SIMP scheme to the motion along field lines raises,

$$u_\parallel^{n+1/2} = u_\parallel^n - \left(\frac{e}{m_e}\tilde{E}_\parallel^n + \mu\frac{dB}{d\zeta}\right)\frac{\Delta t}{2} \tag{12}$$

$$\zeta^{n+1/2} = \zeta^n + u_\parallel^n\frac{\Delta t}{2} \tag{13}$$

$$u_\parallel^{n+1} = u_\parallel^n - \left(\frac{e}{m_e}\tilde{E}_\parallel^{n+1/2} + \mu\frac{\partial B}{\partial\zeta}\right)\Delta t \tag{14}$$

$$\zeta^{n+1} = \zeta^n + \frac{\left(u_\parallel^n + u_\parallel^{n+1}\right)}{2}\Delta t \tag{15}$$

where upper indexes pertain to time discretization. The SIMP scheme requires thus two evaluations of $\tilde{E}$ per time step, at times t^n and $t^{n+1/2}$. For each evaluation, $\tilde{E}_{\|}$ is first calculated on the grid using the discrete counterpart of Eq. (9) and is then interpolated on the electrons, as in regular PIC simulations.

The C++ code was parallelized with OpenMP. Execution on a quad-core multiprocessor allowed a speed-up of 2.6, which corresponds to a parallel efficiency of 65%. Code optimization was mostly governed by the need to remain as long as possible in the parallel region to avoid the large cost of leaving and entering again parallel regions. In order to reduce excessive communication between processors, a separate random number generator and a lightweight copy of the main grid containing a fraction of the electron population is affected to each processor. Only the reduction of the grids to one single grid and the computation of the electric field from data precomputed in the parallel region need to be realized in a single thread. Attention was also paid to reduce as much as possible the size of the data fields to fit the size of cache lines and to keep the whole data set within the L2 cache.

C. Results

1. *Numerical convergence*

Numerical convergence is illustrated using a simulation in slab geometry, starting from somewhat arbitrary initial conditions. As mentioned earlier, the QPIC simulation takes as input the density profile of ions $n_i(\zeta)$, while the density of electrons $n_e(t,\zeta)$ is an output of the model. For illustration purposes, the initial profile $n_e(\zeta, t=0)$ was deliberately chosen so as to break the plasma neutrality at a local level (*i.e.* $n_i \neq n_e$ in each cell), but such that quasineutrality is satisfied at a global level over the whole field line. Figure (2) shows the evolution of the electron density and of the electron temperature over different time scales. Local quasineutrality is recovered over the smallest times scale ($\sim 10^{-7}$ s), after which time the fluctuations of electron density become meaningless, at less than $\pm 2\%$ as can be appreciated from Fig. 3. Figure 2 suggests that the (unphysical) characteristic time scale for this relaxation to local neutrality is of the order of a few wall-to-wall bouncing periods. This is clearly much larger than the physical time scale set by Poisson equation, but would suffice to recover quasineutrality during an ion transport time step in the farther perspective of a combined QPIC-electron/PIC-ion simulation. The temperature stabilizes after $\sim 5 \times 10^{-6}$ s, which roughly corresponds to the relaxation time expected with regards to electrons-neutral collisions. In latter simulations, only this long-term quasi-steady state shall be discussed.

2. *Simulations in slab geometry*

We shall now compare the quasi-steady electric field $E_{\|}$ computed self-consistently to the one estimated from the classical isothermal Boltzmann relation (1) and from the generalized relation (2) proposed by M. Keidar and I. Boyd.[2] Since the goal of such comparison is mainly to assert the accuracy of hybrid models where the isothermal Boltzmann relation is used, the temperature assumed in the case of the Boltzmann and generalized Boltzmann relations is the average of the total temperature $T_e = \frac{1}{3}T_{e\|} + \frac{2}{3}T_{e\perp}$ over the field line.

The simulations of Fig. 4 assume a constant density profile of ion n_{i0} and a shifted parabola for the magnetic field, $B_1(\zeta) = \alpha\zeta^2 + \beta$. The Boltzmann relation raises in this case the trivial solution $E_{\|} = 0$, while the self-consistent formulation expectedly predicts an electric field that would repel ions away from the magnetic mirrors. This effect is significantly over-predicted by the generalized Boltzmann relation, mainly because the average value of T_e over the field line becomes a very poor approximation of $T_{e\perp} - T_{e\|}$ in the region where ∇B is large [compare Eq. (2) and Eq. (3)].

In an ions+electrons simulation, the ion-repelling field of Fig. 4 would eventually deplete the plasma near the walls and result in a density profile with a maximum near the channel centerline. In fact, if one neglected two-dimensional effects altogether and considered that ions move along the simulated field line, the electric field $E_{\|}$ would actually be such that ions are attracted towards the walls in order to satisfy Bohm condition at the sheath edge. For these reasons, and consistently with the typical radial profile of plasma density measured in experiments,[17] the profile $n_{i1}(\zeta)$ of Fig. 1 is considered for the simulations of Fig. 5. Just as in the case of a constant density profile, the Boltzmann relation gives a rather unrealistic estimate of the electric field. Its generalized version provides in this case a better estimate, but remains quantitatively very inadequate. The sign of the electric field and plasma potential shown on Fig. 5 is more consistent with what is usually expected in Hall accelerators.

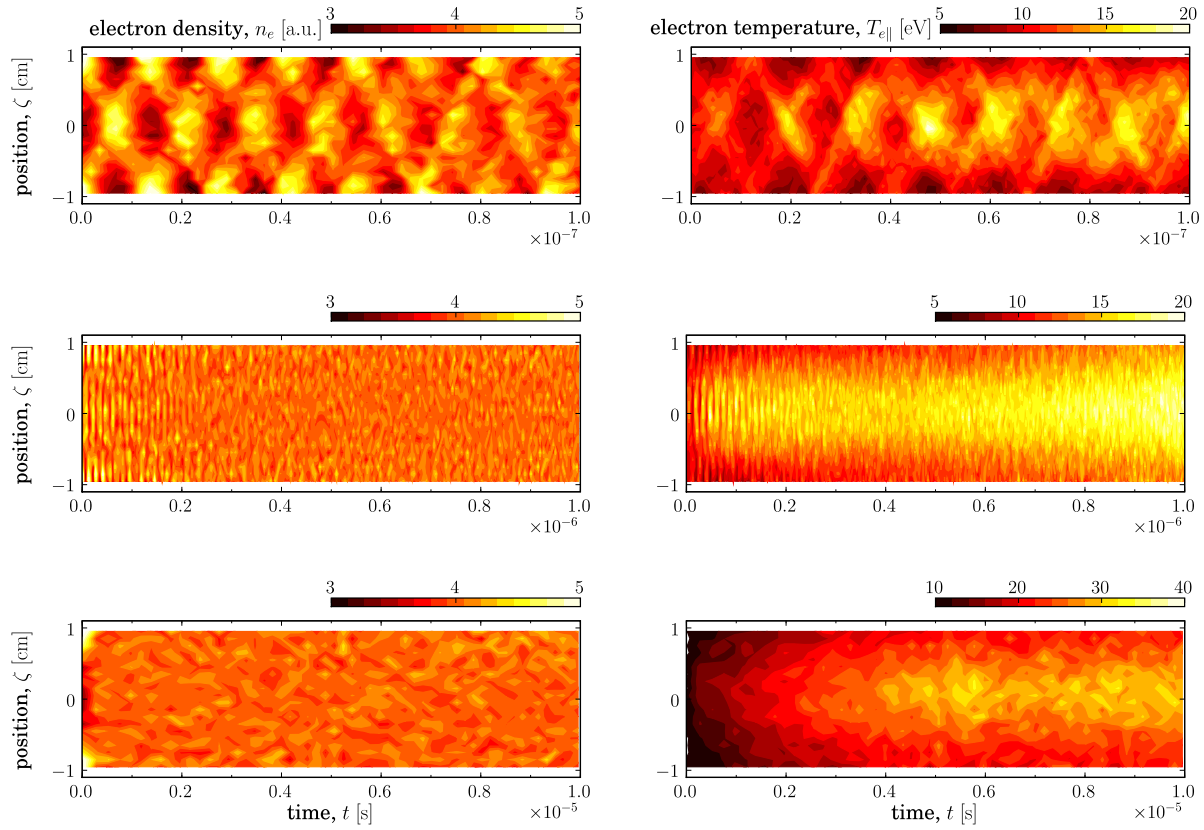

Figure 2: Time evolution of the electron density n_e and temperature $T_{e\|}$ in a slab domain, assuming a constant density of ions $n_i = n_{i0}$ and a symmetric confining magnetic field $B = B_1$.

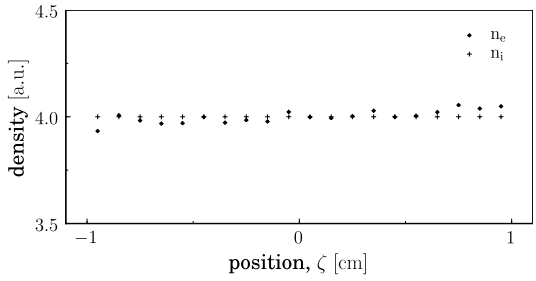

Figure 3: Electron density at time $t = 10^{-5}$ s for the simulation of Fig. 2.

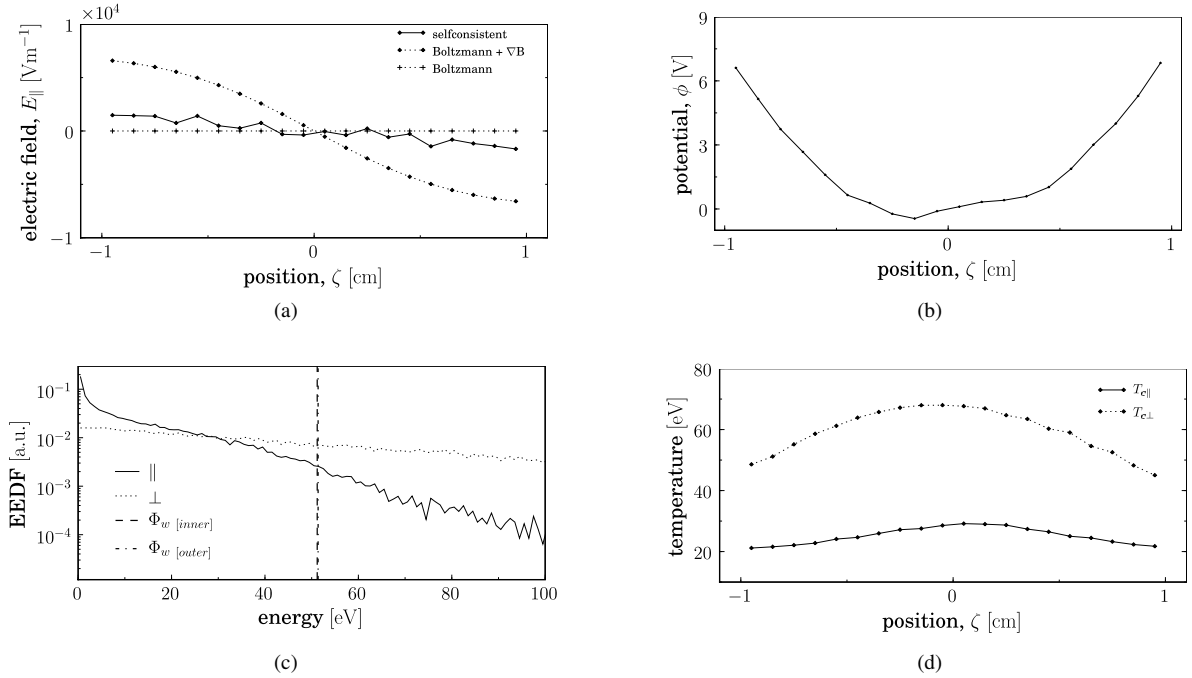

Figure 4: Long term quasi-steady profiles in a slab domain assuming a constant ion density $n_i = n_{i0}$ and a symmetric confining magnetic field $B = B_1$. (a) Comparison between the computed electric field $E_\parallel$ and the prediction from the classical and generalized Boltzmann relations. (b) Plasma potential. (c) Electron energy distribution function. (d) Electron temperature.

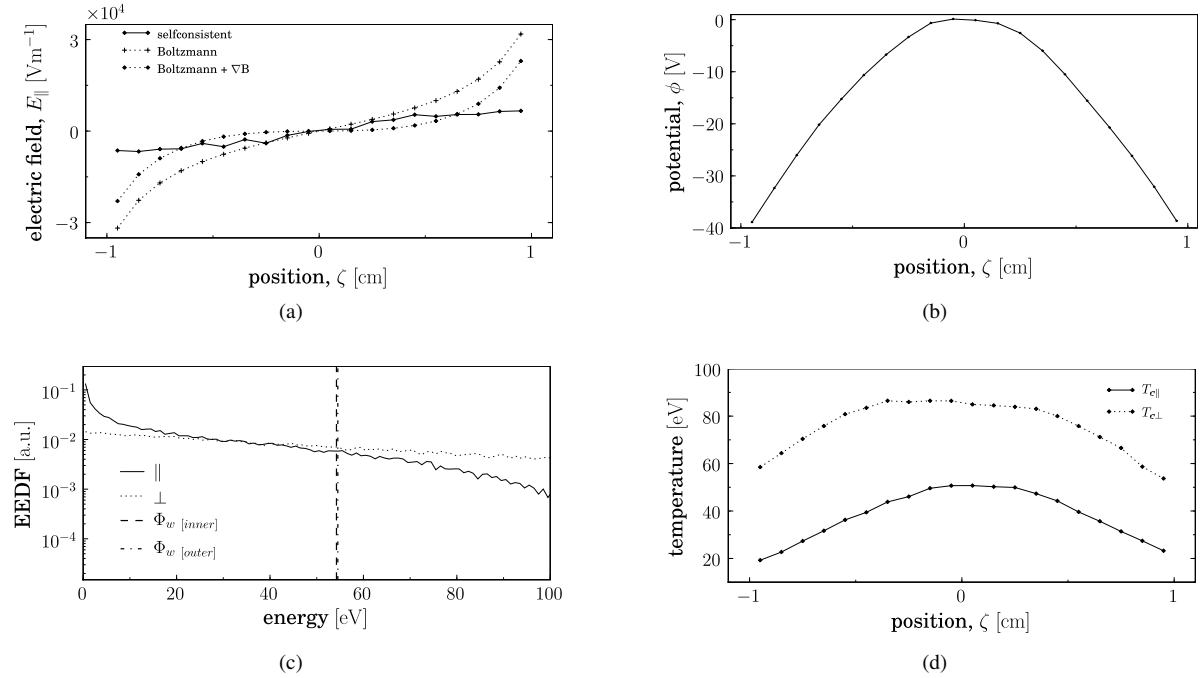

Figure 5:

Long term quasi-steady profiles in a slab domain assuming an ion densityprofile $n_i = n_{i1}$ rarefied near the walls and a symmetric confining magnetic field $B = B_1$. (a) Comparison between the computed electric field $E_\parallel$ and the prediction from the classical and generalized Boltzmann relations. (b Plasma potential. (c) Electron energy distribution function. (d) Electron temperature.

3. *Simulations in axisymmetric geometry*

The quasi-steady results of simulations in an axisymmetric domain without and with magnetic field gradient are shown in Fig. 6 and Fig. 7, respectively. The simulation of Fig. 7 accounts for the typical asymmetry of the divergence-free magnetic field in an axisymmetric domain.

Just as in the case of a slab geometry, the Boltzmann relation and its generalized version[2] give poor estimates for the electric field. Even in the case of a constant magnetic field, the Boltzmann relation strongly overestimates the electric field, due to the fact that the average value of $T_e = \frac{1}{3}T_{e\|} + \frac{2}{3}T_{e\perp}$ on the field line overestimates the value of $T_{e\|}$, particularly at the walls [compare Eq. (1) and Eq. (3)]. Both simulations suggest that the centrifugal force plays at most a marginal role in shaping the electric field.

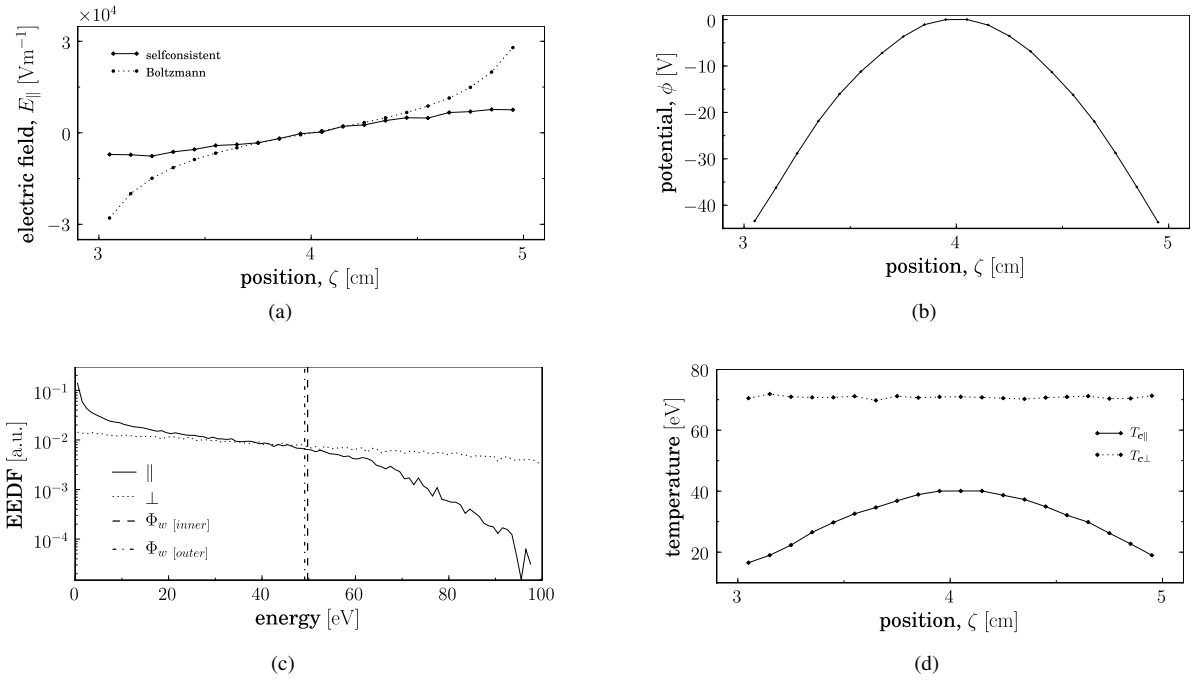

Figure 6: Long term quasi-steady profiles in an axisymmetric domain assuming an ion density profile $n_i = n_{i1}$ rarefied near the walls and a constant magnetic field $B = B_0$. (a) Comparison between the computed electric field $E_\|$ and the prediction from the classical and generalized Boltzmann relations. (b) Plasma potential. (c) Electron energy distribution function. (d) Electron temperature.

IV. Conclusion and perspectives

The QPIC method combined to the guiding center approximation has been successfully tested in one dimension to simulate the dynamics of electrons along a field line in typical Hall thruster conditions and magnetic configurations.

The results obtained thus far suggest that magnetic mirrors provide a dominant contribution to the ambipolar field along the magnetic lines, and that this contribution cannot be reliably estimated with a generalized isothermal Boltzmann relation.[2] The failure of the classical and generalized Boltzmann relations can be attributed to both the large electron pressure anisotropy and to the one-dimensional electron temperature gradient along the field lines. The centrifugal force appears to contribute in a negligible way to the electric field along the magnetic field lines and is largely dominated by the effects of the pressure gradient and magnetic mirror force.

The solver developed in this work is ultimately intended to be used within a 2-dimensional (r, z) simulation for each field line independently, in conjunction with a standard 2D electrostatic PIC solver for ions. In this context, the observation that the QPIC solver achieves approximate local quasineutrality within a few wall-to-wall bouncing periods is important, as it ensures that quasi-neutrality can be in practice recovered between two subsequent time steps of the ion PIC solver. From the implementation side, while the current solver already takes advantage of several fine-grained

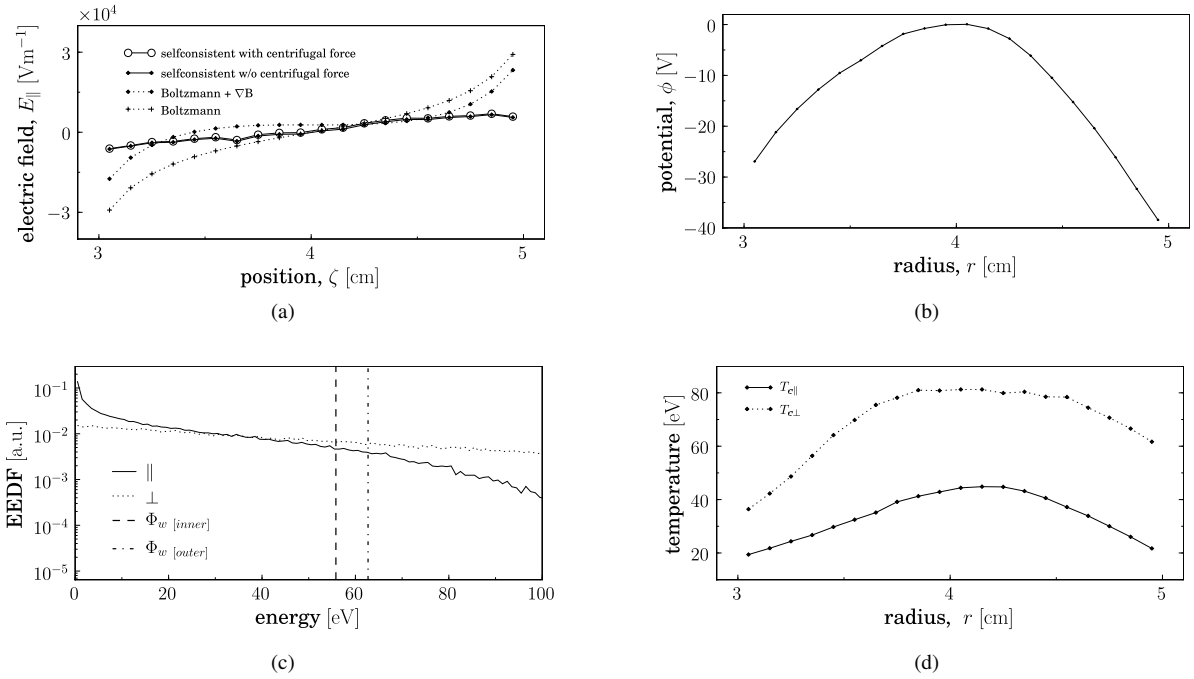

Figure 7: Long term quasi-steady profiles in an axisymmetric domain assuming a density profile $n_i = n_{i1}$ rarefied near the walls and an asymmetric confining magnetic field $B = B_2$. (a) Comparison between the computed electric field $E_\parallel$ (with and without centrifugal force) and the prediction from the classical and generalized Boltzmann relations. (b) Plasma potential. (c) Electron energy distribution function. (d) Electron temperature.

parallelization opportunities to optimize its execution on symmetric multi-processing architectures, simulations in 2 dimensions (*i.e.* with several field lines) will likely require the use of a distributed memory system. Future studies will thus focus on devising a 2D solver allowing coarse-grain parallelization, *i.e.* able to limit the communication overhead incurred by the diffusion of electrons between processors affected to different field lines. Independently of such implementation issues, a more complex physical model of electron-wall interactions and a more exhaustive model of electron-neutral collisions shall be implemented.

Acknowledgments

J. Miedzik is grateful to Snecma for the sponsorship of his MSc and PhD theses.

This work has been performed with funding from the French Research Group "Propulsion par Plasma dans l'Espace" (GDR 3161 CNRS/CNES/SNECMA/Universités).

References

[1]Blinov, N. V., Gorshkov, O. A., and Shagayda, A. A., "Experimental Investigation of Magnetic Field Topology Influence on Structure of Accelerating Layer and Performance of Hall Thruster," *Proc. 29th International Electric Propulsion Conference*, No. 05-033, The Electric Rocket Propulsion Society, Worthington, OH, Princeton, NJ, 2005.

[2]Keidar, M. and Boyd, I. D., "On the Magnetic Mirror Effect in Hall Thrusters," *Appl. Phys. Lett.*, Vol. 87, 2005.

[3]Smirnov, A., Raitses, Y., and Fisch, N. J., "Experimental and Theoretical Studies of Cylindrical Hall Thrusters," *Phys. Plasmas*, Vol. 14, 2007.

[4]Yu, D., Liu, H., Cao, Y., and Fu, H., "The Effect of Magnetic Mirror on Near Wall Conductivity in Hall Thrusters," Vol. 48, 2008, pp. 543.

[5]King, L. B., "A Reexamination of Electron Motion in Hall Thruster Fields," *Proc. 29th International Electric Propulsion Conference*, No. 05-258, The Electric Rocket Propulsion Society, Worthington, OH, Princeton, NJ, 2005.

[6]Lampe, M., Joyce, G., Manheimer, W. M., and Slinker, S. P., "Quasi-Neutral Particle Simulation of Magnetized Plasma Discharges: General Formalism and Application to ECR Discharges," *IEEE. Trans. Plasma Sci.*, Vol. 26, 1998, pp. 1592.

[7]Joyce, G., Lampe, M., and Manheimer, W. M., "Electrostatic Particle-In-Cell Simulation Technique fo Quasi-Neutral Plasma," *J. Comput. Phys.*, Vol. 138, 1997, pp. 540.

[8]Adam, J. C., Héron, A., and Laval, G., "Study of Stationary Plasma Thrusters using Two-Dimensional Fully Kinetic Simulations," *Phys. Plasmas*, Vol. 11, 2004, pp. 295.
[9]Hirakawa, M. and Arakawa, Y., "Particle Simulation of Plasma Phenomena in Hall Thrusters," *Proc. 24th International Electric Propulsion Conference*, No. 95-164, The Electric Rocket Propulsion Society, Worthington, OH, Moscow, 1995.
[10]Szabo, J. J., *Fully Kinetic Numerical Modeling of a Plasma Thruster*, Ph.D. thesis, Massachusetts Institute of Technology, 2001.
[11]Taccogna, F., Longo, S., Capitelli, M., and Schneider, R., "Plasma Flow in a Hall Thruster," *Phys. Plasmas*, Vol. 12, 2005.
[12]Parker, S. E., Procassini, R. J., Birdsall, C. K., and Cohen, B. I., "A Suitable Boundary Condition for Bounded Plasma Simulation without Sheath Resolution," *J. Comput. Phys.*, Vol. 104, 1991, pp. 41.
[13]Taccogna, F., Longo, S., and Capitelli, M., "Plasma Sheaths in Hall Discharge," *Phys. Plasmas*, Vol. 12, 2005.
[14]Phelps, A. V., "Compilation of Collision Cross-Sections for Different Gases," Available at ftp://jila.colorado.edu/collision_data/electronneutral/electron.txt, 1989.
[15]Skullerud, H. R., "The Stochastic Computer Simulation of Ion Motion in a Gas Subjected to a Constant Electric Field," *J. Phys. D*, Vol. 1, 2003, pp. 1567.
[16]Fuchs, V. and Gunn, J. P., "On the Integration of Equations of Motion for Particle-In-Cell Codes," *J. Comput. Phys.*, Vol. 214, 2006, pp. 299.
[17]Bishaev, A. M. and Kim, V., "Local Plasma Properties in a Hall-Current Accelerator with an Extended Acceleration Zone," *Sov. Phys. Tech. Phys.*, Vol. 23, 1979, pp. 1055.